# Exploring the link between cation exchange capacity and magnetic susceptibility

Gaston Matias Mendoza Veirana[1], Hana Grison[2], Jeroen Verhegge[1,3], Wim Cornelis[1], Philippe De Smedt[1,3]

[1]Department of Environment, Faculty of Bioscience Engineering, Ghent University, Coupure Links 653, geb. B, 9000 Ghent, Belgium.
[2] Institute of Geophysics of the Czech Academy of Sciences, Boční II/ 1401, 14100 Prague 4, Czech Republic
[3] Department of Archaeology, Ghent University, Sint-Pietersnieuwstraat 35-UFO, 9000 Ghent, Belgium.

*Correspondence to*: Gaston Matias Mendoza Veirana (Gaston.MendozaVeirana@ugent.be)

**Abstract.** This study explores the relationship between soil magnetic susceptibility ($\kappa$) and cation exchange capacity ($CEC$) across diverse European soils, aiming to enhance pedotransfer functions (PTFs) for soil $CEC$ using near-surface electromagnetic geophysics. We hypothesize that soil $\kappa$, can improve the prediction of $CEC$ by reflecting the soil's mineralogical composition, particularly in sandy soils.

We collected data from 49 soil samples in vertical profiles across Belgium, the Netherlands, and Serbia, including $\kappa$ in-situ conditions ($\kappa_*$~~$\kappa^*$~~), low and high frequency $\kappa$ in the laboratory, in-site electrical conductivity ($\sigma$), iron content, soil texture, humus content, bulk density, water content, water pH, and $CEC$. We used these properties as features to develop univariable and multivariable (in pairs) polynomial regressions to predict $CEC$ for sandy and clayey soils.

Results indicate that $\kappa_*$~~$\kappa^*$~~ significantly improves $CEC$ predictions in sandy soils, independent of clay content, with a combined $\kappa_*$~~$\kappa^*$~~- $\sigma$ model achieving the highest predictive performance ($R^2$ = 0.94). In contrast, laboratory-measured $\kappa$ was less effective, likely due to sample disturbance.

This study presents a novel $CEC$ PTF based on $\sigma$ and $\kappa_*$~~$\kappa^*$~~, offering a rapid, cost-effective method for estimating $CEC$ in field conditions. While our findings underscore the value of integrating geophysical measurements into soil characterization, further research is needed to refine the $\kappa$- $CEC$ relationship and develop a more widely applicable model.

## 1 Introduction

Modern strategies for soil characterization are crucial for addressing the global challenges of soil degradation and pollution. Near-surface electromagnetic geophysics, in particular, facilitates rapid quantitative assessment of soils, offering insights

into subsurface electrical conductivity ($\sigma$), dielectric permittivity ($\varepsilon$), and magnetic susceptibility ($\kappa$) (Garré et al., 2022; Romero-Ruiz et al., 2018). Data collected on these electromagnetic properties can be used for direct qualitative soil survey interpretations or for more comprehensive quantitative analyses involving pedophysical models and pedotransfer functions.

Pedophysical models (PMs) link depth-specific geophysical properties with common soil properties. The need for developing such models is growing due to the demand for high-precision soil characterization (Romero-Ruiz et al., 2018; Verhegge et al., 2021; Wunderlich et al., 2013). Pedotransfer functions (PTFs) are models used to predict soil properties that are typically costly to obtain and are therefore determined less frequently than soil attributes that can be characterized more effectively (Van Looy et al., 2017).

An important indicator of soil health and fertility, which is also crucial in most PMs and PTFs, is the cation exchange capacity ($CEC$) (Glover, 2015; Mendoza Veirana et al., 2023). $CEC$, which refers to a soil's capacity to retain and exchange positively charged ions~~Defined as the ability of a soil to hold and exchange cations~~ (Khaledian et al., 2017), ~~$CEC$~~ is highly correlated with the soil clay content due to a larger colloid surface for particle exchanges. Furthermore, as it is influenced by the soil's physical (e.g., texture), chemical (e.g., pH, mineralogy), and biological properties (e.g., organic matter); thus,~~.~~ $CEC$ integrates aspects from all three main indicator groups commonly used to assess soil quality (Khaledian et al., 2017). Several PMs for soil $\sigma$ prediction include $CEC$ due to the significant influence of free charges on $\sigma$, despite the contribution of other properties such as water content ($\theta$) and salinity or bulk soil $\sigma$ (Glover, 2015). Soil charges can be either permanent or variable, depending primarily on soil pH (Chapman, 1965; Sumner & Miller, 2018). The relationship between clay content and $CEC$ can be highly variable due to its dependence on clay mineralogy (ranging from 3-15 meq/100g for kaolinite to 100-150 meq/100g for vermiculite), and the relative proportion of variable and permanent $CEC$ varies among clay minerals (Miller, 1970; Seybold et al., 2005). To standardize $CEC$ measurements under varying soil conditions, it is common to use the $CEC$ in neutral pH conditions (=7) $CEC7$. However, conventional analytical methods for measuring $CEC$, such as the sodium saturation method, are time-consuming and expensive (Busenberg & Clemency, 1973). Due to the critical importance of $CEC$, its measurement cost, and its correlation with other soil properties, numerous PTFs (Khaledian et al., 2017) and worldwide hybrid models (Poggio et al., 2021) for $CEC7$ have been developed. Commonly, $CEC$ PTFs are expressed in function of clay content and humus, and less frequently pH and soil depth (Khaledian et al., 2017; Seybold et al., 2005). While commonly $CEC$ PTFs are multivariate polynomial regressions, machine learning methods are used in the last decade when large datasets are available, as artificial neural networks (Ghorbani et al., 2015), and genetic expression programming and multivariate adaptive regression splines (Emamgolizadeh et al., 2015). However, when working with small datasets, polynomial regressions are often preferred. Additionally, although~~Although~~ $\sigma$ and $\kappa$ generally correlate well with $CEC$, results have shown that ~~$\sigma$ and soil magnetic susceptibility ($\kappa$)~~ they are independent (Maier et al., 2006).

Soil magnetic susceptibility has been correlated positively with $CEC$ in studies focusing on soil type identification (~~de~~ Mello et al., 2020) (Pearson's correlation 0.4), soil characterization (Siqueira et al., 2010) (Pearson's correlation 0.68),

Field Code Changed

Field Code Changed

Field Code Changed

paleoclimatic reconstruction (Maher, 1998) (Pearson's correlation 0.95 for Podsol and 0.73 for Cambisol samples)., and electromagnetic induction applications (McLachlan et al., 2022). $\kappa$ describes a material's ability to become magnetized when subjected to an external magnetic field. It quantifies the degree of magnetization induced in the substance relative to the strength of the applied magnetic field. The composition of the parent material, and consequently the mineralogy of the rocks and sediments that formed the soils, are the main parameters influencing soil magnetic properties (Jordanova, 2017). Formally, $\kappa$ is defined as $\kappa = \mathrm{H/M}$, where M is the induced magnetization of the material and H is the applied magnetic field. Soil and sediments $\kappa$ measurements are widely used to detect the presence of pedogenic ferrimagnetic minerals (Dearing et al., 1996).

Soil clay content and soil $\kappa$ are correlated positively due to the presence of ferrimagnetic minerals (such as maghemite) in the clay fraction, originating either from the ~~source~~ parent material or through pedogenesis (~~de~~ Mello et al., 2020) (Pearson's correlation 0.26). Consequently, it has been suggested that the observed correlation between $\kappa$ and $CEC$ is actually due to their mutual correlation with clay content, indicating that there may not be a direct effect of $\kappa$ on $CEC$ (~~de~~ Mello et al., 2020).

To the best of our knowledge, the $\kappa$- $CEC$ relationship has not been studied beyond the site level (Siqueira et al., 2010). This limited scope represents a significant research gap, as the broader applicability of $\kappa$ for $CEC$ prediction remain largely unexplored across diverse soil types and conditions.

The main hypothesis is that soil $\kappa$ can support characterizing soil mineralogy, which also influences the permanent component of $CEC$. Therefore soil $\kappa$ may significantly enhance the accuracy of $CEC$ PTFs. This study directly addresses the identified gap by systematically examining the $\kappa - CEC$ relationship using a new comprehensive dataset. The potential to develop more robust, widely applicable $CEC$ PTFs underscores the significance of this work, with implications for sustainable land management, precision agriculture, and environmental monitoring.

To improve predictions of field $CEC$ by integrating soil $\kappa$, this study focuses on ~~we~~ develop and test uni- and multivariate polynomial PTFs based on data of diverse soil types sampled in Europe. In addition, we explore soil $\kappa$ measured in-situ and in laboratory at different frequencies to give insights into the $\kappa$-$CEC$ relationship and investigate how clay content affects the relationship between $\kappa$ and $CEC$. While the methodology of this study focusses on soil and geophysical data collection, data analysis and model development, delving into the underlying physicochemical mechanisms of soil mineralogy that would link $\kappa$ and $CEC$ are out of our scope but is highlighted as an important direction for future research.

To ensure transparency and reproducibility, all the collected data and developed code for this work is publicly available in an open source Python software: (~~(~~Mendoza Veirana, 2024~~)~~).

**Formatted:** Font: Not Italic

**Field Code Changed**

**Field Code Changed**

**Formatted:** Font: Not Bold

**Formatted:** Font: Not Bold

**Field Code Changed**

## 2 Methods

### 2.1 Study area, field measurements, and soil analysis

From 8 sites in Belgium, the Netherlands and Serbia, 49 soil samples were collected across a wide range of USDA soil textures from sand to clay, and WRB (IUSS Working Group WRB, 2022) soil types (Figure 1 and Table 1, see also Mendoza Veirana et al. (2023)). Specifically, 6 sites in Belgium contributed 38 samples, one site in the Netherlands contributed 6 samples, and one site in Serbia contributed 5 samples. This distribution ensures representation of diverse soil types and textures across the three countries. At each site, test pits were dug to identify and sample different soil horizons. For each soil horizon and within a vertical soil profile, soil field $\kappa$ was measured ($\kappa_s$) (5 to 11 measurements per site, 49 in total) using a kappa meter SM30 (ZH Instruments, Brno, Czech Republic) at 8 kHz. The sensor measures soil $\kappa$ with a penetration depth of 2 cm and a sensitivity of $10^{-7}$ SI units. First, the sensor was placed against the soil's profile wall for a measurement, followed by an additional measurement taken in open air away from the profile to obtain a reference zero $\kappa$ value for measurement calibration (ZH instruments, 2022). Additionally, a HydraProbe sensor (Stevens, Water Monitoring Systems) was employed to measure $\sigma$ along the profile wall. The correction proposed by Logsdon et al. (2010) was applied to improve the quality of these readings.

Undisturbed soil samples (100 cm³) were collected manually, by pushing standard steel rings horizontally into the soil profile wall at the same locations where $\kappa_s$ was measured. After the cores were weighed fresh and oven-dried for 24 h at 105 °C, volumetric water content ($\theta$) was calculated from the water-mass loss divided by the core volume, and bulk density ($b_d$) from the oven-dry mass divided by the same volume (Grossman and Reinsch, 2002).

Disturbed soil samples of about 250 g were collected around the undisturbed samples. They were air-dried, homogenized in an agate mortar, and sieved using a 2 mm mesh for determination of texture, and chemical and magnetic soil properties. Clay, silt and sand content (denoted as Clay, Silt, Sand, respectively, expressed in %) was measured following the pipette method (NF X31-107, 2003) ~~ISO 11464~~after sieving at 2 mm, content of humus, $CEC$ was determined by CoHex method (Ciesielski et al., 1997a, 1997b).

Formatted: Font: Not Bold

Formatted: Font: (Default) +Body (Times New Roman)

Formatted: Font: (Default) +Body (Times New Roman)

Formatted: Font: (Default) +Body (Times New Roman)

Formatted: Font: (Default) +Body (Times New Roman)

Formatted: Font: (Default) +Body (Times New Roman)

Formatted: Font: Not Bold

Formatted: Font: (Default) +Body (Times New Roman)

Formatted: Font: (Default) +Body (Times New Roman)

Formatted: Font: (Default) +Body (Times New Roman)

Formatted: Font: (Default) +Body (Times New Roman)

Formatted: Font: (Default) +Body (Times New Roman)

115

| | Samples | Soil type | Depth [cm] | *Sand* [%] | *Clay* [%] | $\kappa_*$ [$10^{-5}$] | $\kappa_{lf}$ [$10^{-5}$] | $\kappa_{fd}$ [-] | *Fe* [ppm] | *Humus* [%] | $\sigma$ [mS/m] | $CEC$ [meq/ 100g] |
|---|---|---|---|---|---|---|---|---|---|---|---|---|
| A | 5 | Luvisols | [4,106] | [9,16] | [9,13] | [14,32] | [14,40] | [5.2,8.1] | [14,21] | [0.1,2.3] | [12,35] | [6,9] |
| DREN | 5 | | [72,252] | [18,35] | [27,39] | [47,66] | [51,70] | [6.2,9.1] | [31,38] | [0.6,1.6] | [30,53] | [20,25] |
| E | 5 | Cambisols | [20,110] | [24,35] | [20,25] | [7.2,14] | [8,15] | [3.5,5.5] | [19,25] | [0.8,2.6] | [38,50] | [9,12] |
| EH2 | 5 | Phaeozems | [20,94] | [10,54] | [17,53] | [12,20] | [13,38] | [3.2,6.7] | [42,50] | [0.3,5.7] | [55,66] | [16,39] |
| HOEKE | 11 | Cambisols | [28,258] | [9,45] | [16,32] | [4.5,116] | [6.8,127] | [4.4,8.1] | [17,34] | [0.5,11] | [27,59] | [8,30] |
| P | 7 | Retisols | [32,144] | [42,80] | [8,11] | [2.6,12] | [4.5,16] | [2.9,8.5] | [5.9,12] | [0,2] | [8,17] | [1.6,11] |
| S | 5 | Arenosols | [28,130] | [83,93] | [5,7] | [3,20] | [2.9,73] | [3.3,9.2] | [3.6,16] | [0,2] | [11,29] | [2,5] |
| VALTHE | 6 | Podzol | [10,60] | [91,95] | [3,4] | [0.8,12] | [1.2,19] | [3.9,9.7] | [1,2.5] | [0,2.2] | [0.5,1] | [1.6] |
| All | 49 | | [4,252] | [9,95] | [3,53] | [0.8,116] | [1.2,127] | [2.9,9.7] | [1,50] | [0,11] | [0,66] | [1.6,39] |

**Table 1 Minimum and maximum intervals of soil and magnetic properties for each explored site. Data ranges reflect the diversity of soil types and conditions across various sites.**

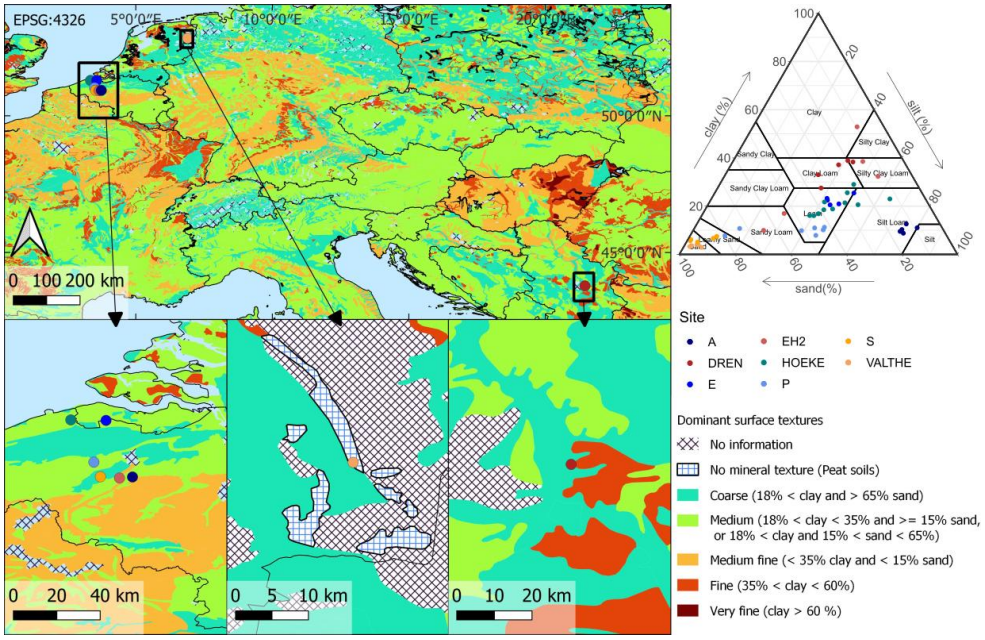


**Figure 1 Locations of the study sites. Background shows dominant surface texture (European Soil Database v2.0, 2004). Colors represent the texture of the sites: sandy in yellowish, silty in blueish and clayey in reddish. The United States Department of Agriculture (USDA) texture triangle showing the particle size distribution categorized by sampling site. The samples presented in Table 1 are represented by triangles (adapted from (Mendoza Veirana et al., 2023)).**

Magnetic susceptibility $\kappa$ was measured using a Kappabridge MKF1-FA (AGICO Instruments, Brno, Czech Republic), in addition to the field $\kappa$ measurements. Prior to these laboratory measurements, corrections were made to eliminate the influence of the diamagnetic sample holder. Samples were placed in 10 $cm^3$ plastic holders, and the in-phase $\kappa$ was recorded at both low frequency ($\kappa_{lf}$) and high frequency ($\kappa_{hf}$) (976 Hz and 15616 Hz, respectively). Thus, the percentage frequency dependent magnetic susceptibility ($\kappa_{fd}$) was calculated as:

$$\kappa_{fd} = \frac{\kappa_{lf} - \kappa_{hf}}{\kappa_{lf}} \times 100 \ [\%]$$

**Equation 1**

Additionally, the absolute difference ($\kappa_{fd\,abs} = \kappa_{lf} - \kappa_{hf}$) was calculated. Such measurements are used to detect the presence of superparamagnetic ferrimagnetic minerals occurring as ultrafine (<0.03 μm) crystals (mostly ultrafine magnetite and maghemite) produced largely by pedogenic biochemical processes in soil (Dearing, 1994). Samples where ultrafine minerals are present will show increased frequency dependent magnetic susceptibility; samples without such minerals will show identical $\kappa$ values at the two frequencies.

To support magnetic observations, elemental analyses were performed to evaluate the total iron content concentration (Fe) of all samples through X-ray fluorescence (XRF, Niton XL3t GOLDD+, Thermo Fisher Scientific Inc., USA) on samples that passed a 0.5 mm sieve and placed in capsules covered with $4^{-6}$ m cellophane. Three consecutive XRF measurements were performed and averaged for each sample.

**2.2 Model development**

~~Developing a $CEC$ PTF using soil $\kappa$ data that can be generalized beyond site-specific is a challenging task, requiring careful consideration of the data used for model development.~~ The absence of previous attempts at developing a $CEC$ PTF using soil $\kappa$ data that can be generalized beyond site-specific ~~this~~ highlights the importance of thorough data exploration. We chose to build polynomial models due to their interpretability, simplicity, and the use of only one tuning parameter (polynomial degree), which is suitable given the relatively small dataset (n=49).

Field and laboratory measured soil properties were used as features for predicting $CEC$ (target variable), these are: soil depth, water pH, $Humus$, $Clay$, $Silt$, and $Sand$, $b_d$, $\sigma$, $\kappa_*$, $\kappa_{lf}$, $\kappa_{fd}$, $\kappa_{fd\,abs}$, and $Fe$. All (13) features were used to develop univariable polynomial regressions, and multivariable models were created by combining features in pairs, resulting in 91 feature combinations. The top four combinations in terms of test performance were compared to the standard combination of *Clay* and *Humus* content, also, single features were considered ($Clay$, $\sigma$, and $\kappa_*$).

Since model performance was largely dependent on clay content, the samples were divided into sandy (n=25) and clayey (n=24) groups, using the median clay content (16.1%) as a threshold. Both input datasets were split randomly into training (70%) and testing (30%) subsets, without consideration of any soil characteristics. This approach ensured that samples from different sites, soil horizons, and physicochemical properties were mixed during data splitting. To further ensure an unbiased model evaluation, the training and testing process was repeated 100 times. The best polynomial degree (linear or quadratic) was determined by the highest median of the $R^2$ test scores over the 100 repetitions (Tibshirani et al., 2001). Finally, model implementation was performed after tuning and feature selection using all the samples of each subset.

Formatted: Font: Italic

### 2.3 Statistical analysis

Predicting $CEC$ based on soil properties, particularly focusing on magnetic characteristics is a multivariate problem. Commonly, many variables are linearly correlated with $CEC$, such as *Clay*, $\kappa$, *Fe*, *Humus*, and $\sigma$. The challenge lies in distinguishing between independent and masked effects. Importantly, the positive correlation between $\kappa$ and $CEC$ may be due to the strong correlation between clay content and both $CEC$ and $\kappa$ (~~de~~ Mello et al., 2020).

Field Code Changed

To address this, we quantified the independent correlation between $\kappa$ and $CEC$, irrespective of the effects of clay by calculating the partial correlation, that is the correlation between the residuals of the linear fitting of the covariable (*Clay*) with the variables ($\kappa$ and $CEC$).

## 3 Results and discussion

### 3.1 Data exploration

A general variable exploration analysis is presented in this section, which is fundamental for the model development in the next section. Spearman's rank correlations between all the features mentioned and target can be seen in Figure 2. As expected, soil $\kappa$ is less correlated to $CEC$ than common soil properties such as *Clay* and *Sand*, water pH and $\theta$, while *Fe* and $\sigma$ correlate strongly with $CEC$. Additionally, consistent with the findings of ~~de~~ Mello et al. (2020) and Ayoubi et al. (2018), there is a positive correlation between *Clay* and $\kappa$ (both $\kappa_*$ and $\kappa_{lf}$). Also in line with Maier et al. (2006), $\sigma$ is not correlated significantly to $\kappa$. Conversely, *Sand* correlates negatively with both $\kappa$ and *Fe*.

Field Code Changed

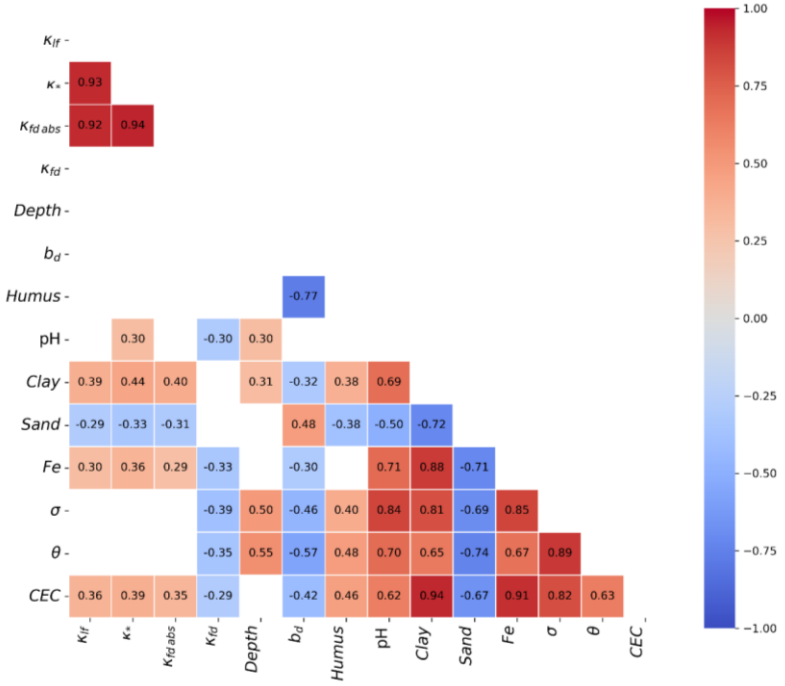


**Figure 2 Spearman rank correlation heatmap showing significant P-values≤0.005 for the 49 soil samples, missing correlations have P-values>0.005.**

Comparing soil $\kappa_*$ to $\kappa_{lf}$ reveals a similar trend across the entire range of observations ($10^{-5}$ to $10^{-3}$) (see Figure 3). This trend persists despite $\kappa_*$ being measured in undisturbed soil structures with field bulk density, while $\kappa_{lf}$ was obtained from repacked samples that do not preserve the field structure and density. Additionally, the measurement frequency for $\kappa_*$ (8 kHz) differs from that of $\kappa_{lf}$ (~1 kHz).

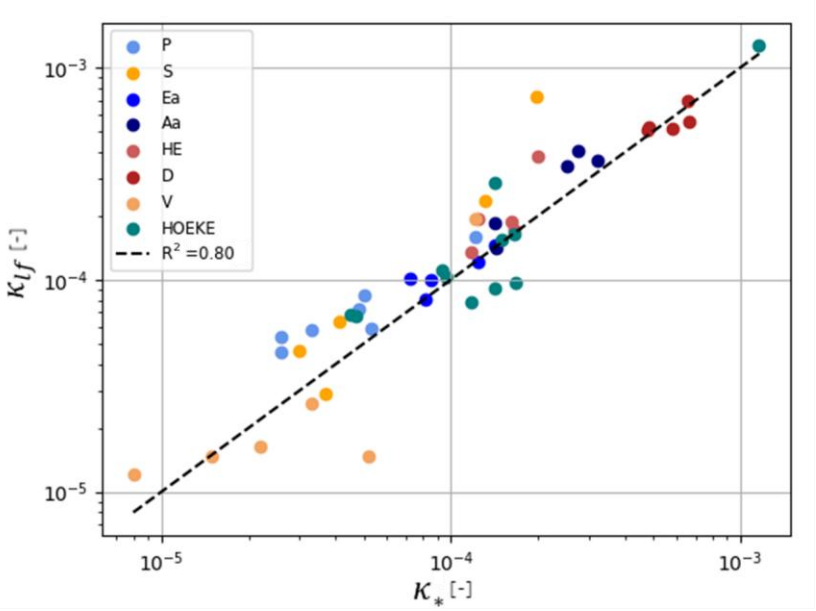


**Figure 3 Logarithmic scatter plot showing the ~~field~~ in-situ obtained ~~observed~~ magnetic susceptibility ($\kappa_*$) vs the laboratory observed low frequency magnetic susceptibility ($\kappa_{lf}$).**

### 3.2 $CEC$ modelling

Model training and testing was performed in sandy and clayey groups independently. The predictors for $CEC$, with the best overall model performance, turned out to be highly dependent on the group. Notably, using $\sigma$ and $\kappa_*$ provided the best prediction results on the sandy group, with training and testing median $R^2$ values of 0.95 and 0.85, respectively (see Figure 4). This performance is significantly higher than that achieved with the commonly used features, such as *Clay* and *Humus* content, which had a median test $R^2$=0.38. Additionally, the combination of *Sand* and *pH* performed equally well, followed closely by combinations of $\kappa_*$ and $\kappa_{lf}$ features.

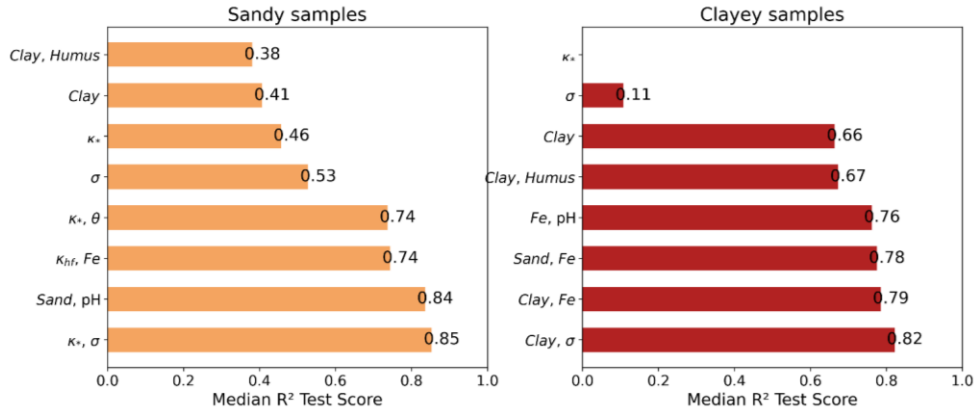


**Figure 4 Horizontal bar plot showing test model performances of $CEC$ prediction based on different features (vertical axis) for sandy and clayey samples. Features shown here are the top four in performance (bottom), and $\kappa_*$, $\sigma$, Clay, and the pair Clay, Humus.**

The strong performance of $\sigma$ and $\kappa_*$ as predictors of $CEC$ in sandy soils (median test $R^2 = 0.85$) is particularly noteworthy. $\sigma$ is known to be influenced by several factors including soil water content, salinity, and the concentration of dissolved ions, which collectively can reflect the variable component of $CEC$ (Glover, 2015). In sandy soils, which typically have lower water and nutrient retention capacities, $\sigma$ can provide a dynamic measure of the available exchangeable cations at a given time. Concurrently, the strong predictive capacity of $\kappa_*$ suggests it captures a different, yet complementary, aspect of $CEC$. In soils with low clay content, and therefore limited colloid surface area, the permanent component of $CEC$ is likely more affected by minerals. The fact that $\kappa_*$ measured in-situ, performed better than laboratory $\kappa$ suggests that the undisturbed soil structure and field conditions are crucial for this relationship, possibly reflecting the spatial arrangement and contact of these minerals within the soil matrix.

Additionally, both $\sigma$ and $\kappa_*$ can be quickly measured in field conditions without the need for invasive sampling. Therefore, after implementing the best $CEC$ PTF for sandy samples (see Figure 5):

$$CEC = 1.233 + 14000 \cdot \kappa_* - 0.00861 \cdot \sigma - 5.91 \cdot 10^7 \cdot {\kappa_*}^2 + 1350 \cdot \kappa_* \cdot \sigma + 0.000624 \cdot \sigma^2;\ R^2 = 0.94$$

**Equation 2**

Where $\kappa_*$ is unitless, $\sigma$ is in mS/m and $CEC$ in meq/100g .



**Formatted:** Font: (Default) +Body (Times New Roman)
**Formatted:** Font: (Default) +Body (Times New Roman)
**Formatted:** Font: (Default) +Body (Times New Roman)
**Formatted:** Font: (Default) +Body (Times New Roman)
**Formatted:** Font: (Default) +Body (Times New Roman), Not Bold
**Formatted:** Font: (Default) +Body (Times New Roman)
**Formatted:** Font: (Default) +Body (Times New Roman), Not Bold
**Formatted:** Font: (Default) +Body (Times New Roman)
**Formatted:** Font: (Default) +Body (Times New Roman)
**Formatted:** Font: (Default) +Body (Times New Roman), Not Bold
**Formatted:** Font: (Default) +Body (Times New Roman), Not Bold
**Formatted:** Font: (Default) +Body (Times New Roman), Not Bold, Not Italic
**Formatted:** Font: (Default) +Body (Times New Roman), Not Bold, Not Italic
**Formatted:** Font: (Default) +Body (Times New Roman), Not Bold, Not Italic
**Formatted:** Font: (Default) +Body (Times New Roman), Not Bold, Not Italic
**Formatted:** Font: (Default) +Body (Times New Roman), Not Bold
**Formatted:** Font: (Default) +Body (Times New Roman), Not Bold
**Formatted:** Font: (Default) +Body (Times New Roman), Not Bold, Italic
**Formatted:** Font: (Default) +Body (Times New Roman), Not Bold
**Formatted:** Font: (Default) +Body (Times New Roman)
**Formatted:** Font: (Default) +Body (Times New Roman)
**Formatted:** Font: (Default) +Body (Times New Roman)
**Formatted:** Font: (Default) +Body (Times New Roman)
**Formatted:** Font: (Default) +Body (Times New Roman)
**Formatted:** Font: (Default) +Body (Times New Roman)
**Formatted:** Font: (Default) +Body (Times New Roman)

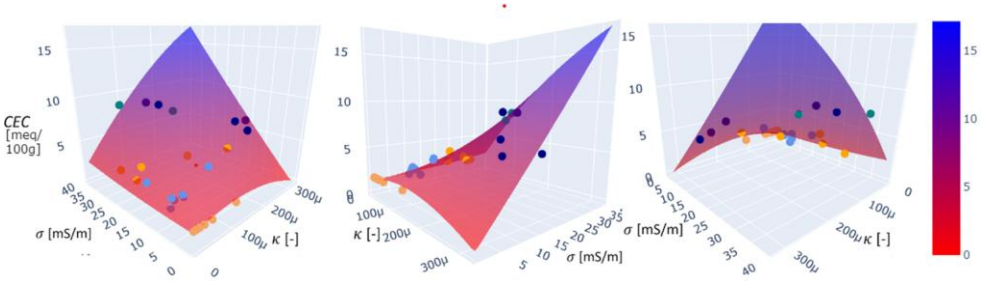


**Figure 5 Implemented $CEC$ PTF for sandy samples (clay<16.1) (Equation 2) with a $R^2$=0.94. The model is colored in vertical axis from red to blue to visualize its shape. Colored dots represent the samples used in the sandy group, belonging to different sites that match the colors in Figure 1.**

For clayey samples, $\sigma$ and *Clay* features resulted in the best performance with a training and testing $R^2$ equal to 0.89 and 0.82, respectively. This result is in line with the literature since the link between $CEC$, $\sigma$ and *Clay* is well documented (Glover, 2015; Wunderlich et al., 2013). For clayey samples, $\kappa$ was not an outstanding feature, likely due to the influence of larger colloid surface that may not be effectively characterized by $\kappa$ .

### 3.3 $\kappa_*$- $CEC$ statistics

The partial correlation between $\kappa_*$ and $CEC$, while controlling for (removing the effect of) *Clay*, was found to be 0.61 for sandy samples, and -0.14 for clayey samples. This indicates that in sandy samples, $\kappa_*$ is just partially influenced by *Clay*. For clayey samples, however, $\kappa_*$ is heavily influenced by the soil's clay content, making the correlation between $\kappa_*$ and $CEC$ minor if the effect of *Clay* is removed. Consequently, predicting $CEC$ using *Clay* alone is as effective as using both *Clay* and $\kappa_*$ (median testing $R^2$ of 0.66 and 0.64, respectively), while $\kappa_*$ alone is a poor predictor (see Figure 4).

## 4 Limitations and further directions

The current study, while providing novel insights, has several limitations that also point towards important future research directions.

Formatted: Font: (Default) +Body (Times New Roman)
Formatted: Font: (Default) +Body (Times New Roman)
Formatted: Font: (Default) +Body (Times New Roman)
Formatted: Font: (Default) +Body (Times New Roman)
Formatted: Font: (Default) +Body (Times New Roman)
Field Code Changed
Formatted: Font: (Default) +Body (Times New Roman)
Formatted: Font: (Default) +Body (Times New Roman)
Formatted: Font: (Default) +Body (Times New Roman)
Formatted: Font: (Default) +Body (Times New Roman)
Formatted: Font: (Default) +Body (Times New Roman)
Formatted: Font: (Default) +Body (Times New Roman)
Formatted: Font: (Default) +Body (Times New Roman)
Formatted: Font: Not Bold

Firstly, ~~T~~the main limitation~~s~~ of the analyzed results are related to the dataset size, although diverse in terms of European soil types, is relatively small. A~~; a~~ larger sample size could improve the statistical relevance of the findings and improve the robustness and generalizability of the developed PTFs (Van Looy et al., 2017). Future work should aim to expand the database with more samples covering an even wider range of soil properties and parent materials.

Secondly, all collected samples come from non-tropical regions, where organic matter content and bacterial activity do not significantly influence soil $\kappa$. In contrast, these factors may contribute substantially to higher soil $CEC$ in other environments (Seybold et al., 2005). Therefore, the results are valid for the sampled sites that belong to European soils, and applications to scenarios beyond this range of soils should be approached with caution.

Thirdly, a significant limitation is the lack of direct mineralogical analysis, especially for clay and iron oxide fractions. While $\kappa$ offers an indirect proxy for ferrimagnetic mineralogy, detailed characterization (e.g., via X-ray diffraction) is needed for a mechanistic understanding of the $\kappa$-$CEC$ link. Identifying specific clay minerals (like kaolinite vs. smectite) and their abundance would clarify their $CEC$ contributions and interactions with magnetic minerals. This is a crucial step to move beyond empirical correlations towards a process-based understanding

Fourthly, while field-measured $\kappa$ proved useful, the reasons for its superiority over laboratory-measured $\kappa_{lf}$ or $\kappa_{fd}$ in the PTFs warrant further exploration. This could involve investigating the effects of soil structure, moisture content (which are preserved in in-situ $\kappa$ measurements). A deeper understanding of how these factors influence different $\kappa$ measurements could lead to optimized measurement strategies.

Finally, the model shown in Equation 2 is valid for samples with clay content between 2.9% to 16.1%, $\sigma$ between 0.55 mS/m to 39 mS/m, $\kappa_*$ between 8 to 320 μ, and $CEC$ between 1.6 meq/100g to 8.7 meq/100g.

As larger and more comprehensive datasets become available, exploring advanced modelling techniques, such as machine learning algorithms, may capture more complex, non-linear relationships. Assessing the scalability of the $\kappa$-$CEC$ relationship from point measurements to field-scale predictions using proximal sensing platforms, for example, vehicle-mounted EMI sensors providing dense $\kappa$ data (McLachlan et al., 2022), would be beneficial.

## 5 Conclusions

For the first time, the link between soil $\kappa$ and $CEC$ has been explored using data that extends beyond the site level. By analyzing soil samples across Europe, encompassing a range of diverse soil physicochemical properties, we found that $\kappa_*$ significantly contributes to predicting soil $CEC$, particularly in sandy samples, and this contribution is linearly independent of the soil clay content. Conversely, soil $\kappa$ measured in the laboratory was less effective, likely due to the disturbance of soil structure and soil density.

Based on these findings, we proposed a novel PTF for $CEC$ in sandy samples, with a $R^2$ of 0.94, based on $\sigma$ and $\kappa_*$, which likely relate to the variable and permanent components of $CEC$, respectively. This PTF is valuable because both $\sigma$ and $\kappa_*$ are

Formatted: Font: Not Bold
Formatted: Font: Not Bold
Formatted: Space After: 0 pt
Formatted: Font: Not Bold
Formatted: Font: Not Bold
Formatted: English (United Kingdom)
Formatted: Font: Not Italic
Formatted: Font: Not Italic
Formatted: Font: Not Italic
Formatted: Font: Not Italic
Formatted: Font: Not Italic
Formatted: Font: Not Italic
Formatted: Font: Not Italic
Formatted: Font: Not Italic
Formatted: Font: Not Italic
Formatted: Space After: 0 pt
Formatted: Font: Not Bold
Formatted: Font: Not Bold
Formatted: Font: Not Bold
Formatted: Font: Not Bold
Formatted: Font: Not Bold
Formatted: Font: Not Bold

quick and inexpensive to measure in the field, making it straightforward to predict $CEC$ under field conditions. For instance, it can be used to quickly assess the fertility of sandy soils across agricultural fields.

Further research, along with expanding the existing database, could enhance $CEC$ modeling and provide deeper insights into the $\kappa_*$- $CEC$ relationship. These advances could help integrate independent geophysical properties such as $\sigma$ and $\kappa$, to quantify key soil properties like $CEC$, advancing a more holistic approach towards soil characterization.

**Data availability**

10.5281/zenodo.13971643

**Code availability**

https://github.com/orbit-ugent/kappa-CEC

**Author contribution**

PS, MV and JV designed the surveys and carried them out. MV developed the model code and performed the simulations and contributed to statistical formal analysis along HG. JV, HG, PS and WC gave writing advice. MV prepared the manuscript with contributions from all co-authors.

**Competing interests**

The authors declare that they have no conflict of interest.

**Special issue statement**

Agrogeophysics: illuminating soil's hidden dimensions

**Acknowledgements**

Text readability and code performance were boosted by using generative AI (Chat-GPT 4o, OpenAI)

**References**

Ayoubi, S., Mohsen Jabbari, & Hossein Khademi. (2018). Multiple linear modeling between soil properties, magnetic susceptibility and heavy metals in various land uses. *Modeling Earth Systems and Environment (2018) 4:579–589 Https://Doi.Org/10.1007/S40808-018-0442-0*, *4*, 579–589. https://doi.org/10.1007/s40808-018-0442-0

Busenberg, E., & Clemency, C. V. (1973). Determination of the Cation Exchange Capacity of Clays and Soils Using an Ammonia Electrode. *Clays and Clay Minerals*, *21*(4), 213–217. https://doi.org/10.1346/CCMN.1973.0210403

Chapman, H. D. (1965). Cation-Exchange Capacity. In A. G. Norman (Ed.), *Agronomy Monographs* (pp. 891–901). American Society of Agronomy, Soil Science Society of America. https://doi.org/10.2134/agronmonogr9.2.c6

Ciesielski, H., Sterckeman, T., Santerne, M., & Willery, J. P. (1997a). A comparison between three methods for the determination of cation exchange capacity and exchangeable cations in soils. *Agronomie*, *17*(1), 9–16. https://doi.org/10.1051/agro:19970102

Ciesielski, H., Sterckeman, T., Santerne, M., & Willery, J. P. (1997b). Determination of cation exchange capacity and exchangeable cations in soils by means of cobalt hexamine trichloride. Effects of experimental conditions. *Agronomie*, *17*(1), 1–7. https://doi.org/10.1051/agro:19970101

Dearing, J. A. (1994). *Environmental Magnetic Susceptibility. Using the Bartington MS2 system*.

Dearing, J. A., Hay, K. L., Baban, S. M. J., Huddleston, A. S., Wellington, E. M. H., & Loveland, P. J. (1996). Magnetic susceptibility of soil: An evaluation of conflicting theories using a national data set. *Geophysical Journal International*, *127*(3), 728–734.

Emamgolizadeh, S., Bateni, S. M., Shahsavani, D., Ashrafi, T., & Ghorbani, H. (2015). Estimation of soil cation exchange capacity using Genetic Expression Programming (GEP) and Multivariate Adaptive Regression Splines (MARS). *Journal of Hydrology*, *529*, 1590–1600. https://doi.org/10.1016/j.jhydrol.2015.08.025

**Formatted:** Bibliography, Widow/Orphan control, Adjust space between Latin and Asian text, Adjust space between Asian text and numbers

Garré, S., Blanchy, G., Caterina, D., De Smedt, P., Romero-Ruiz, A., & Simon, N. (2022). Geophysical methods for soil applications. In *Reference Module in Earth Systems and Environmental Sciences*. Elsevier. https://doi.org/10.1016/B978-0-12-822974-3.00152-X

Ghorbani, H., Kashi, H., Hafezi Moghadas, N., & Emamgholizadeh, S. (2015). Estimation of Soil Cation Exchange Capacity using Multiple Regression, Artificial Neural Networks, and Adaptive Neuro-fuzzy Inference System Models in Golestan Province, Iran. *Communications in Soil Science and Plant Analysis*, *46*(6), 763–780. https://doi.org/10.1080/00103624.2015.1006367

Glover. (2015). Geophysical Properties of the Near Surface Earth: Electrical Properties. In *Treatise on Geophysics* (pp. 89–137). Elsevier. https://doi.org/10.1016/B978-0-444-53802-4.00189-5

IUSS Working Group WRB. (2022). *World Reference Base for Soil Resources. International soil classification system for naming soils and creating legends for soil maps* (4th edition). IUSS. https://wrb.isric.org/files/WRB_fourth_edition_2022-12-18.pdf

Jordanova, N. (2017). *Soil Magnetism. Applications in Pedology, Environmental Science and Agriculture*. Academic Press.

Khaledian, Y., Brevik, E. C., Pereira, P., Cerdà, A., Fattah, M. A., & Tazikeh, H. (2017). Modeling soil cation exchange capacity in multiple countries. *CATENA*, *158*, 194–200. https://doi.org/10.1016/j.catena.2017.07.002

Logsdon, S. D., Green, T. R., Seyfried, M., Evett, S. R., & Bonta, J. (2010). Hydra Probe and Twelve-Wire Probe Comparisons in Fluids and Soil Cores. *Soil Science Society of America Journal*, *74*(1), 5–12. https://doi.org/10.2136/sssaj2009.0189

Maher, B. A. (1998). Magnetic properties of modern soils and Quaternary loessic paleosols: Paleoclimatic implications. *Palaeogeogr Palaeoclimatol Palaeoecol*, *137*(1–2), 25–54.

Maier, G., Scholger, R., & Schön, J. (2006). The influence of soil moisture on magnetic susceptibility measurements. *Journal of Applied Geophysics*, *59*(2), 162–175.

McLachlan, P., Schmutz, M., Cavailhes, J., & Hubbard, S. S. (2022). Estimating grapevine-relevant physicochemical soil zones using apparent electrical conductivity and in-phase data from EMI methods. *Geoderma*, *426*, 116033. https://doi.org/10.1016/j.geoderma.2022.116033

Mello, D., Demattê, J. A. M., Silvero, N. E. Q., Di Raimo, L. A. D. L., Poppiel, R. R., Mello, F. A. O., Souza, A. B., Safanelli, J. L., Resende, M. E. B., & Rizzo, R. (2020). Soil magnetic susceptibility and its relationship with naturally occurring processes and soil attributes in pedosphere, in a tropical environment. *Geoderma*, *372*, 114364. https://doi.org/10.1016/j.geoderma.2020.114364

Mendoza Veirana. (2024). *orbit-ugent/kappa-CEC: First release* (Version 0.1) [Computer software]. Zenodo. https://doi.org/10.5281/ZENODO.13970660

Mendoza Veirana, G., Verhegge, J., Cornelis, W., & De Smedt, P. (2023). Soil dielectric permittivity modelling for 50 MHz instrumentation. *Geoderma*, *438*, 116624. https://doi.org/10.1016/j.geoderma.2023.116624

Miller, W. F. (1970). Inter-regional predictability of cation-exchange capacity by multiple regression. *Plant and Soil*, *33*(1–3), 721–725. https://doi.org/10.1007/BF01378263

Poggio, L., De Sousa, L. M., Batjes, N. H., Heuvelink, G. B. M., Kempen, B., Ribeiro, E., & Rossiter, D. (2021). SoilGrids 2.0: Producing soil information for the globe with quantified spatial uncertainty. *SOIL*, *7*(1), 217–240. https://doi.org/10.5194/soil-7-217-2021

Romero-Ruiz, A., Linde, N., Keller, T., & Or, D. (2018). A Review of Geophysical Methods for Soil Structure Characterization: Geophysics and soil structure. *Reviews of Geophysics*, *56*(4), 672–697. https://doi.org/10.1029/2018RG000611

Seybold, C. A., Grossman, R. B., & Reinsch, T. G. (2005). Predicting Cation Exchange Capacity for Soil Survey Using Linear Models. *Soil Science Society of America Journal*, *69*(3), 856–863. https://doi.org/10.2136/sssaj2004.0026

Siqueira, D. S., Marques Jr, J., Matias, S. S. R., Barrón, V., Torrent, J., Baffa, O., & Oliveira, L. C. (2010). Correlation of properties of Brazilian Haplustalfs with magnetic susceptibility measurements: Magnetic susceptibility in Brazilian Haplustalfs. *Soil Use and Management*, *26*(4), 425–431. https://doi.org/10.1111/j.1475-2743.2010.00294.x

Sumner, M. E., & Miller, W. P. (2018). Cation Exchange Capacity and Exchange Coefficients. In D. L. Sparks, A. L. Page, P. A. Helmke, R. H. Loeppert, P. N. Soltanpour, M. A. Tabatabai, C. T. Johnston, & M. E. Sumner (Eds.), *SSSA Book Series* (pp. 1201–1229). Soil Science Society of America, American Society of Agronomy. https://doi.org/10.2136/sssabookser5.3.c40

Tibshirani, R., Friedman, J., & Hastie, T. (2001). *The Elements of Statistical Learning: Data Mining, Inference, and Prediction*. Springer.

Van Looy, K., Bouma, J., Herbst, M., Koestel, J., Minasny, B., Mishra, U., Montzka, C., Nemes, A., Pachepsky, Y. A., Padarian, J., Schaap, M. G., Tóth, B., Verhoef, A., Vanderborght, J., van der Ploeg, M. J., Weihermüller, L., Zacharias, S., Zhang, Y., & Vereecken, H. (2017). Pedotransfer Functions in Earth System Science: Challenges and Perspectives. *Reviews of Geophysics*, *55*(4), 1199–1256. https://doi.org/10.1002/2017RG000581

Verhegge, J., Mendoza Veirana, G., Cornelis, W., Crombé, P., Grison, H., De Kort, J.-W., Rensink, E., & De Smedt, P. (2021). Working the land, searching the soil: Developing a geophysical framework for Neolithic land-use studies. Project introduction,-methodology, and preliminary results at 'Valther Tweeling.' *Notae Praehistoricae*, *41*, 187–197.

Wunderlich, T., Petersen, H., Hagrey, S. A. al, & Rabbel, W. (2013). Pedophysical Models for Resistivity and Permittivity of Partially Water-Saturated Soils. *Vadose Zone Journal*, *12*(4), vzj2013.01.0023. https://doi.org/10.2136/vzj2013.01.0023

ZH instruments. (2022). *Magnetic susceptibility meter SM-30. User's manual.* http://www.zhinstruments.com/assets/sm-30-manual.pdf